Reports in Mechanical Engineering
Vol. 7, No. 1, 2026, pp. 169-184
ISSN: 2683-5894, DOI: https://doi.org/10.31181/rme575

Mechanical Process Control and Statistical Process Control for Reducing Butter-Oil Defects in Industrial Production

Suresh Kumar Sahani[1], Ravi Kumar Raj[2], K. Sathishkumar[3], G N Keshava Murthy[4], Manojkumar S B[5], Naveen K B[5], Binod Kumar Sah[6], A. Jayanthiladevi[5], Pintu Mandal[1], Kameshwar Sahani[7*]

[1]Faculty of Science, Technology, and Engineering, Rajarshi Janak University, Janakpurdham, Nepal
[2]Department of Management, Rajarshi Janak University, Janakpurdham, Nepal
[3]Assistant Professor, PG and Research Department of Computer Science, Erode Arts and Science College (Autonomous), Erode – 638009, Tamil Nadu, India
[4]Electronics and Instrumentation Engineering Department, Siddaganga Institute of Technology, Tumakuru
[5]Department of ECE, BGS Institute of Technology, Adichunchanagiri University, B G Nagara, Mandya, Karnataka, India
[6]R.R.M.C., T.U., Nepal
[7]Department of Civil Engineering, School of Engineering, Kathmandu University, Dhulikhel, Nepal

Article Info

Article history:

Received November 17, 2025
Revised December 15, 2026
Accepted February 14, 2026

Keywords:

Reliability, Availability,
Butter-Oil Processing,
Serial Process,
Markov Analysis,
Mean Time between Failures (MTBF),
Mean Time to Repair (MTTR)

ABSTRACT

This study provides a quantitative assessment of the reliability and availability of a serial butter-oil manufacturing line from a mechanical engineering perspective. The line comprises critical rotating and fluid-handling subsystems raw-milk receiving pumps, cream separators, heat exchangers, mechanical agitators, homogenizers, gearboxes, and conveying components whose mechanical integrity profoundly impacts throughput and quality. We characterize the production train using continuous-time Markov chains (CTMCs) based on a reliability block diagram (RBD) that depicts series dependencies and maintenance plans. Component-level failure (λ) and repair (μ) rates, derived from realistic duty cycles and mechanical failure modes (bearing wear, seal leakage, misalignment, lubrication starvation, cavitation, fouling, and thermomechanical fatigue), are conveyed to system-level metrics via state-transition analysis. Numerical simulations yield mean time between failures (MTBF), mean time to repair (MTTR), and steady-state availability for the entire system and for mechanically essential subsystems (pump-valve assemblies and homogenization units). Sensitivity analyses identify availability limitations and priorities mechanical factors bearing L10 lifespan, seal mean time between failures, lubricant replacement interval, alignment tolerance, and cooling-water temperature differential according to their impact on throughput decrease. The results suggest that minor improvements in repair logistics for high-criticality assets (such as the use of cartridge seals and quick-release couplings on feed pumps) might exceed substantial reductions in MTBF for low-criticality components. We demonstrate that the integration of mechanical condition monitoring (vibration and temperature trending) with SPC-based run charts and control limits stabilizes essential mechanical variables (overall vibration, RMS acceleration, and discharge pressure ripple), thereby reducing special-cause variation and unanticipated downtime. The study concludes with maintenance strategies for mechanical assets, encompassing spares pooling for prevalent failure categories, precision alignment, optimized lubrication practices, and threshold-based, condition-directed overhauls, yielding measurable improvements in line availability and energy efficiency while upholding butter-oil quality standards.

Corresponding Author:

Kameshwar Sahani
Department of Civil Engineering, School of Engineering, Kathmandu University, Dhulikhel, Nepal
Email: sahanikmh093@gmail.com

1. Introduction

Centrifugal separation, heat treatment, mechanical agitation, homogenization, pumping, and conveyance affect throughput, energy consumption, and product quality in commercial butter-oil production. An unexpected stoppage on a serial manufacturing line may turn off upstream and downstream units, increasing rework and operating costs. Mechanical engineers' main challenge is to quantify how component failures (bearings, seals, couplings, shafts, valves) and repair dynamics affect line-level performance, and to identify the few crucial actions that increase steady output.

Traditional food and process reliability studies employ block-diagram, queuing, or general Markov chains to estimate uptime. However, two holes remain. Initially, numerous studies ignored mechanical failure modes (e.g., lubricant hunger, misalignment, cavitation, seal wear, thermal-mechanical fatigue) and the associated repair profiles, thereby limiting their relevance to maintenance and design teams. Second, Statistical Process Control (SPC) is widely used for product variables. Still, its integration with mechanical condition indicators (overall vibration, RMS acceleration, bearing temperature, discharge-pressure ripple) precursors to special-cause variation and potential downtime is lacking. The butter-oil line is a series of mechanically linked machines that handle fluids in specific ways. These machines include centrifugal separators, positive-displacement pumps, gearboxes, agitators, homogenizers, and clarifiers. They are all connected by pipes, valves, and conduits. The integrity of the bearings and seals, the alignment of the components, the level of lubrication, and the vibration behavior of these assets are the mechanical health indicators that directly impact the throughput, energy consumption, and product quality. That being said, the butter-oil manufacturing line is best understood as a fixable mechanical system in which total availability is determined by how well and reliably its essential spinning equipment is maintained.

Mechanical engineering emphasizes availability and maintainability because wear-out processes, stochastic disturbances, and maintenance limitations constrain performance in modern systems. Availability is the fraction of calendar time during which the system is operable (excluding maintenance). Maintainability is the probability of restoring it to its specified operating state within a given time after failure, shaped by design-for-service features, spare-parts logistics, and preventive/corrective maintenance policies in Markov/RBD models of repairable systems (Garg & Sharma, 2012; Ramírez-Rosado & Bernal-Agustín, 2001; Uprety, 2012; Verma & Chari, 1991). Managers use availability allocation and reliability optimization to apportion targets across components and minimize life-cycle costs in complex mechanical assets, using metaheuristics and exact methods. The Grey Wolf Optimizer (GWO) family has delivered competitive results across both constrained and unconstrained single- and multi-objective problems (network siting, learning systems, power dispatch, and transmission economics). No single optimizer can address all reliability and availability concerns, per the no-free-lunch theorem. This has evolved to hybrid and problem-specific techniques (Wolpert & Macready, 1997). These methods are supplemented by solution techniques for nonlinear systems, particle swarm optimization (PSO) (and MOPSO), cuckoo search algorithm (CSA), and decomposition methods for large-scale mechanical engineering systems like power and transportation networks. (Baskan, 2013; Buaklee & Hongesombut, 2013; dos Santos Coelho, 2009; Eberhart & Kennedy, 1995; Li & Haimes, 1992). In this context, butter-oil (clarified butter) production is executed by a serial train of mechanical process units raw-milk reception and positive-displacement pumping; centrifugal separation/clarification; thermal conditioning via plate/tubular heat exchangers; mechanical agitation and phase handling; high-pressure homogenization; buffer/holding with level-controlled pumping; polishing/finishing; and packaging/dispatch—interlinked by valves, piping, and conveyance; because the architecture is serial, downtime in a bottleneck mechanical asset (often the separator–pump train) can idle the entire line, so system-level performance depends critically on the availability and maintainability of rotating equipment and thermal-fluid components, which our mechanically informed Markov/RBD framework addresses through failure (λ) and repair (μ) modeling, MTBF/MTTR/availability computation, sensitivity analysis, and cost-aware availability allocation and redundancy planning (Baskan, 2013; Buaklee & Hongesombut, 2013; dos Santos Coelho, 2009; Eberhart & Kennedy, 1995; Garg & Sharma, 2012; Li & Haimes, 1992; Mirjalili et al., 2014; Mirjalili et al., 2016; Ramírez-Rosado & Bernal-Agustín, 2001; Uprety, 2012).

This study creates a mechanically informed serial butter-oil manufacturing line reliability-availability architecture to address these issues. We create a reliability block diagram (RBD) of the production train using a continuous-time Markov chain (CTMC) to capture component-level failure and repair rates, to calculate system-level MTBF, MTTR, and steady-state availability, and to priorities components and mechanical parameters based on their impact on line performance. We examine how combining SPC with condition monitoring may stabilize critical mechanical variables and reduce special-cause losses without hardware changes.

(1) A plant-realistic RBD-CTMC model that preserves mechanical failure-mode structure (bearings, seals, alignment, and lubrication) rather than aggregating units into generic blocks.

(2) Quantification of mean time between failures, mean time to repair, and availability for the serial line and key subsystems such separator–pump trains and homogenization modules.

(3) Sensitivity and criticality rating that identifies availability bottlenecks and compares repair-time savings to MTBF advantages to inform maintenance design decisions such cartridge seals, quick-release couplings, and access clearances.

(4) Integrating mechanical and statistical process control to regulate vibration, temperature, and pressure ripple metrics to decrease variation due to unique sources and avoid unexpected stoppages.

This research treats the RBD-CTMC formulation as a mechanical reliability model that transfers the failure (λ) and repair (μ) rates at the component level into system-level metrics including MTBF, MTTR, and steady-state availability. In mechanical reliability engineering, this is the norm; using these models, decision-makers choose how much redundancy to implement, how often to do maintenance, and how to handle overhauls for rotating gear. The framework also helps interpret SPC alarms and vibration trends as indicators of mechanical health, informing condition-based maintenance thresholds and repair priorities. It does this by linking CTMC states and transition rates to condition-monitoring indicators, such as overall vibration levels, RMS acceleration, bearing temperature, and discharge-pressure ripple.

The examination of system dependability and optimization has progressed from traditional analytical frameworks to sophisticated stochastic and computational intelligence methodologies. Verma and Chari (Verma & Chari, 1991) conducted preliminary foundational research on system failures in common-cause shock situations, whereas Li and Haimes (Li & Haimes, 1992) introduced decomposition methodologies for large-scale reliability optimizations. Garg and Sharma (Garg & Sharma, 2012) expanded upon research on behavioral and performance-based systems. Later, Upreti (Uprety, 2012) developed stochastic and probabilistic modelling methods that performed well for industrial systems, using the Chapman–Kolmogorov equations and Laplace transform methods. As systems got more complicated, evolutionary and swarm intelligence approaches became more popular. Eberhart and Kennedy (Eberhart & Kennedy, 1995) developed Particle Swarm Optimization (PSO), which opened a new area of optimization research. Wolpert and Macready (Wolpert & Macready, 1997) subsequently discussed its theoretical limits. Coelho (dos Santos Coelho, 2009), Kumar (Kumar et al., 2013), and Negi et al. (Negi et al., 2021) made further progress in PSO-based frameworks for dependability and nonlinear optimization. Cuckoo Search (Baskan, 2013; Buaklee & Hongesombut, 2013) and the Flower Pollination Algorithm are two more metaheuristic methods that have also been shown to perform well in reliability-redundancy and engineering optimization. Mirjalili et al. (Mirjalili et al., 2014) introduced the Grey Wolf Optimizer (GWO), which has become a widely used nature-inspired optimization technique. Its multi-objective extension (Mirjalili et al., 2016), together with improved versions such as chaotic GWO (Kohli & Arora, 2018) and refraction-learning-based upgrades (Long et al., 2019), has greatly improved exploration and convergence. GWO has been extensively utilized in several fields, including power system optimization, (Gupta & Saxena, 2016; Kamboj et al., 2016; Ramírez-Rosado & Bernal-Agustín, 2001), wireless sensor networks (Fouad et al., 2015), signal processing and classification tasks (Manikandan et al., 2016; Mosavi et al., 2016), image thresholding (Li et al., 2016), and UAV route planning (Zhang et al., 2016). Research on hybrid and economic dispatch applications can be found in Jayabarathi et al., (Jayabarathi et al., 2016) have written extensively on reliability - cost optimization studies using GWO. Thorough evaluations by Negi et al. (Negi et al., 2021) substantiate the growing significance of GWO and other metaheuristic methodologies in reliability engineering.-The literature unequivocally demonstrates a paradigm shift from deterministic analytical techniques to intelligent hybrid optimization methodologies, in which the Grey Wolf Optimizer and other metaheuristic algorithms are crucial for addressing contemporary dependability and industrial engineering challenges. Garg and Sharma (Garg & Sharma, 2012) and Kumar (Kumar et al., 2013) focused on the dependability and behavioral analysis of industrial systems using analytical and soft computing methodologies. Mosavi et al. (Mosavi et al., 2016) showed that hybrid neural networks enhanced by the Grey Wolf Optimizer performed well in classification tests. Mirjalili et al. (Mirjalili et al., 2014) developed the Grey Wolf Optimizer, a popular metaheuristic algorithm inspired by nature. Wolpert and Macready (Wolpert & Macready, 1997) formulated the No Free Lunch theorem, emphasizing that no single optimization strategy is uniformly superior. Mirjalili et al., (Mirjalili et al., 2016) made important contributions to the development of metaheuristic and particle swarm optimization methods for solving nonlinear, multi-objective, and reliability optimization problems. These methods improved convergence, accuracy, and system performance in complex engineering applications.

The study is based on the assumption that the operating circumstances are statistically stationary, with independent exponential time-to-failure and repair. Within this scope, the methodology proposes high-leverage maintainability and monitoring interventions that can be applied quickly and assessed quantitatively. When applied to other mechanically demanding food processing lines with serial dependencies, the technique may be transferred seamlessly.

1.1 Reception and Processing of Milk

Diverse contractors and milk collection locations transport milk to the plant dock using milk tankers towed by leased vehicles. The primary elements of this activity are unloading and grading. Assessment, analysis, and assessment

of milk specimens. Raw milk is stored in silos after being chilled to 4°C in milk chillers, which are fed from the dump tank, thereby enhancing its storage quality. Subsequently, the raw milk is chilled and processed by the milk plate pasteurizer, a standalone apparatus that warms and cools the milk. After being heated to 4-45 degrees Celsius, the milk is transferred to a cream separator, where the cream is extracted. The skimmed milk is then returned to the milk pasteurizer, where it is heated to 80 degrees Celsius to guarantee its safety for human consumption. Ultimately, it is chilled to 4 degrees Celsius to enhance its storage quality.

2. Removing Fat from Milk

The milk that has been pasteurized at a temperature of 45 degrees Celsius is sent to the cream separator, where the fat is extracted from the milk in the form of cream that contains between 40 and 50 percent fat. The skimmed milk produced is then returned to the milk pasteurizer.

3. The Process of Cold-Pressured Cream

To pasteurize cream, one must heat each particle to at least 71°C. To prepare the pasteurized cream for subsequent processing into butter and butter-oil, it is held in a double-jacketed tank. To make churning feasible, cream is cooled and aged by reducing its temperature and kept for a few hours.

4. Production of Butter

The cream is transferred from the storage tank to the butter churner. The cream is processed in the machine to produce butter granules. Buttermilk is extracted individually and pumped back into the raw milk silos, while the butter granules are further processed in the machine to produce a homogeneous butter mass. The butter is extracted from the machine and sent to melting vats by butter carts.

5. Producing Butter-Oil

After the butter has melted in the vats, it is transferred to the butter-oil boiler and gradually heated to 107° C to remove any water vapor. After that, it is left undisturbed for a few hours to finish melting. After being pumped out of the boiler, the butter-oil is sent to settling tanks to settle for a few hours. This process removes the tiny particles of residue from the butter-oil. Once clarified, the butter-oil is transferred to a storage tank and chilled to a temperature (between 28 and 30 degrees Celsius) that is ideal for filling.

6. Butter-Oil Containers

The quality control team tests the butter oil stored in the tank for a variety of parameters, then packs it into tins of varying sizes after analysis. An illustration of the flowchart depicting the process of producing butter-oil can be seen in Figure 1.

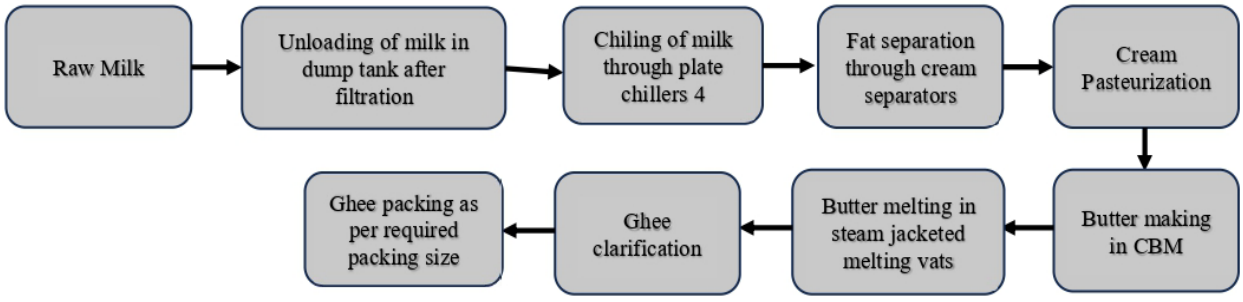

Figure 1: Flow Diagram of Butter-Oil Manufacturing Plant

7. Notations and Systems

According to the information presented in this chapter, the production plant for butter oil is comprised of the following eight sub-systems.

7.1 Sub-System 1 (Pumping)

The most important component of the plant is the one responsible for unloading milk brought in from the numerous milk collection centers. A flawless switchover mechanism has been used to bring two pumps online, one operational and the other in standby mode. As a result, we have thought that this component of the system is completely reliable.

7.2 Sub-System 2 (Chiller)

A vital component of the plant, this is, too. We assume that the plant's backup chiller, which is always on standby, likewise never fails.

7.3 Sub-System S_1 (Separator)

Centrifugal force is the fundamental mechanism that enables this plant component to operate. The milk is refrigerated in the chiller and thereafter sent to the cream separator, where it is transformed into cream with 40-50% fat. The skimmed milk is thereafter stored in silos for conversion into milk powder. The motor, bearings, and high-speed gearbox are the three primary components that operate in succession.

7.4 Sub-System S_2 (Pasteurizer)

This component guarantees that the separator's cream is pasteurized. To pasteurize the cream, the temperature must reach 71°C throughout the cream. In practice, when heated to 80-82°C, there is no holding time. Its aims include killing off dangerous bacteria, removing off-putting flavor components, rendering enzymes inactive, and eradicating undesirable infections. This subsystem may also be used to remove the tanning chemicals from the cream. The pasteurized cream is stored in a double-jacketed tank for further processing. In a reduced form, it may operate thanks to its series-connected motor and bearings.

7.5 Sub-System S_3 (Continuous Butter Making)

The cream storage tank supplies the CBM, which then pumps the cream out. The butter particles are produced by churning the cream using this apparatus. After being pumped to raw milk silos, the butter granules undergo further processing in the machine to form a homogeneous mass, which is the final result of the technique. The homogenized butter is then moved to the melting vats using butter carts. The CBM consists of a gearbox, motor, and a set of bearings.

7.6 Sub-System S_4 (Melting Vats)

The component that makes up this system is a storage tank that has two covers. To remove the water, the butter is heated to around 107°C and then allowed to cool. The next step is to let the melted butter cool for about half an hour, untouched. This subsystem consists of series-connected motors, bearings, and monoblock pumps.

7.7 Sub-System S_5 (Butter-Oil Clarifier)

The butter-oil is transferred to the settling tanks after melting in the vats, where it settles for a few hours before being carried on to the next stage. Then, as a final step, the butter oil is sent to storage tanks after any residual bits are filtered out. We can now maintain the butter-oil at a temperature between 28°C and 30°C. In this specific subsystem, the gearbox and the motor are connected in series.

7.8 Sub-System S_6 (Packaging)

This part of the system uses a pouch-filling machine to make the processed butter-oil packets. The machine knows how to fill, flow, and seal automatically. The pneumatic cylinder and printed circuit board are connected in series in this subsystem.

To keep things simple, we'll look at the first two of the six subsystems.

7.9 Added Notes

Alongside the designations for sub-systems, namely S_1, S_2, S_3, S_4, and S_5, we have employed the subsequent notations.

1. $\overline{S_2}$ Shows that sub-system S_2 is operating in a diminished condition.
2. λ_1, λ_2, λ_3, λ_4, λ_5, and λ_6 stands for the subsystems' respective constant failure rates S_1, S_3, S_4, S_5, S_6, $\overline{S_2}$ and S_2
3. μ_1, μ_2, μ_3, μ_4, μ_5, and μ_6 indicate, respectively, the rates of repair that are constant for the subordinate system S_1, S_3, S_4, S_5, S_6, and S_2
4. $f_1(t)$, $f_2(t)$, …, $f_{13}(t)$ determined the probability that were associated with the systems at the moment t.

5. X_1, X_2, X_3, X_4, X_5, and X_6 represent the failed state of the sub-systems S_1, S_2, S_3, S_4, S_5, and S_6, respectively.

7.10 Presumptions

1. The rates of failure and repair are not dependent on one another, and the unit of measurement for both is per day.

II. No subsystems can fail at the same time.
III. Only through a reduced state does the sub-system S2 fail.
IV. In the same way that the new components work, the repaired ones do as well.
V. Standby systems' switchover devices are faultless.

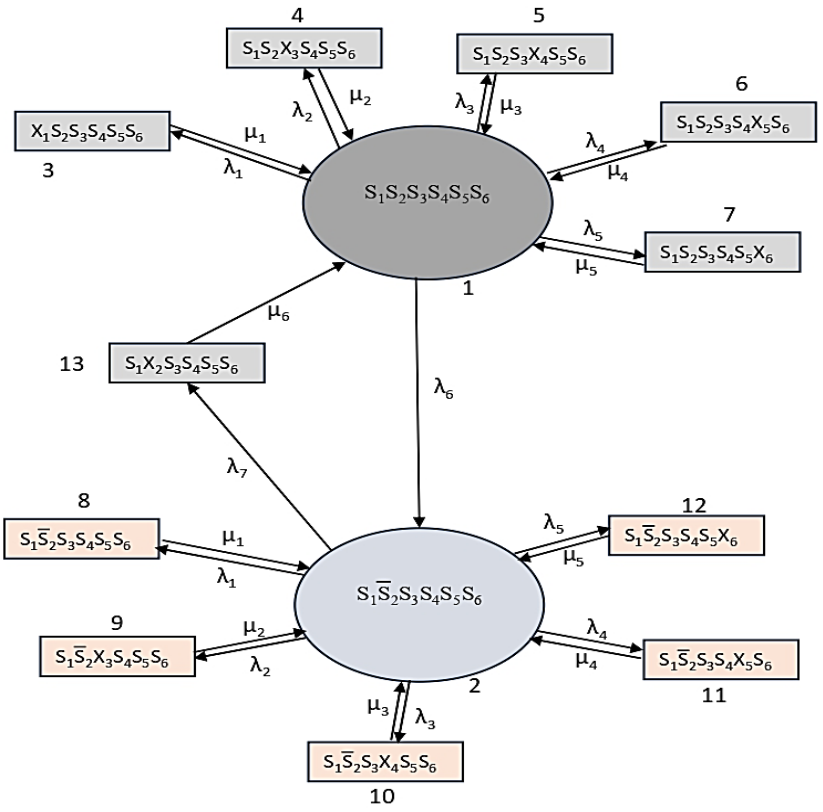

Figure 2: Butter Oil Production Facility Transition Diagram

8. Mathematical Representation of the System

8.1 Short-Term State

Based on probability, the following set of first-order differential equations and the system's transition map are linked.

$$\frac{df_1(t)}{dt} + (\lambda_1+\lambda_2+\lambda_3+\lambda_4+\lambda_5+\lambda_6)\, f_1(t) = \mu_1 f_3(t) + \mu_2 f_4(t) + \mu_3 f_5(t) + \mu_4 f_6(t) + \mu_5 f_7(t) + \mu_6 f_{13}(t) \quad (1)$$

$$\frac{df_2(t)}{dt} + (\lambda_1+\lambda_2+\lambda_3+\lambda_4+\lambda_5+\lambda_7)\, f_2(t) = \mu_1 f_8(t) + \mu_2 f_9(t) + \mu_3 f_{10}(t) + \mu_4 f_{11}(t) + \mu_5 f_{12}(t) + \lambda_6 f_1(t) \quad (2)$$

$$\frac{df_3(t)}{dt} + \mu_1 f_3(t) = \lambda_1 f_1(t) \quad (3)$$

$$\frac{df_4(t)}{dt} + \mu_2 f_4(t) = \lambda_3 f_1(t) \quad (4)$$

$$\frac{df_5(t)}{dt} + \mu_3 f_5(t) = \lambda_3 f_1(t) \quad (5)$$

$$\frac{df_6(t)}{dt} + \mu_4 f_6(t) = \lambda_4 f_1(t) \quad (6)$$

$$\frac{df_7(t)}{dt} + \mu_5 f_7(t) = \lambda_5 f_1(t) \quad (7)$$

$$\frac{df_8(t)}{dt} + \mu_1 f_8(t) = \lambda_1 f_2(t) \quad (8)$$

$$\frac{df_9(t)}{dt} + \mu_2 f_9(t) = \lambda_2 f_2(t) \quad (9)$$

$$\frac{df_{10}(t)}{dt} + \mu_3 f_{10}(t) = \lambda_3 f_2(t) \quad (10)$$

$$\frac{df_{11}(t)}{dt} + \mu_4 f_{11}(t) = \lambda_4 f_2(t) \quad (11)$$

$$\frac{df_{12}(t)}{dt} + \mu_5 f_{12}(t) = \lambda_5 f_2(t) \quad (12)$$

$$\frac{df_{13}(t)}{dt} + \mu_6 f_{13}(t) = \lambda_7 f_2(t) \quad (13)$$

With the boundary condition

$$f_m(0) = 1 \text{ if } m = 1 \text{ and } f_m(0) = 0 \text{ if } m \neq 1 \quad (14)$$

Equation (14) includes boundary conditions that have been solved using the Rk-4 technique for the system of differential equations (1) to (13) with those conditions. For various subsystem failure rates and repair options, numerical companions have been run from time t = 0 to t = 360 days.

The system's dependability R (t) may be calculated by

$$R(t) = f_1(t) + f_2(t) \quad (15)$$

8.2 Permanent Condition

Management is often concerned with the system's long-term availability in sectors such as goods processing. We need the system's steady-state probabilities to determine its long-run availability. Obtaining the probability of the systems in their steady state may be accomplished by setting the following restrictions:

$$\frac{d}{dt} \to 0 \text{ as } (t) \to \infty .$$

In this situation, equations (1) through (13) may be reduced to the equations that are presented below.

Again, we made use of the symbols f_1, f_2, f_3, f_{13} as $t \to \infty$.

Then

$$(\lambda_1+\lambda_2+\lambda_3+\lambda_4+\lambda_5+\lambda_6) f_1 = \mu_1 f_3 + \mu_2 f_4 + \mu_3 f_5 + \mu_4 f_6 + \mu_5 f_7 + \mu_6 f_{13} \quad (16)$$

$$(\lambda_1+\lambda_2+\lambda_3+\lambda_4+\lambda_5+\lambda_7) f_2 = \mu_1 f_8 + \mu_2 f_9 + \mu_3 f_{10} + \mu_4 f_{11} + \mu_5 f_{12} + \lambda_6 f_1 \quad (17)$$

$$\mu_1 f_3 = \lambda_1 f_1 \quad (18)$$

$$\mu_2 f_4 = \lambda_2 f_1 \quad (19)$$

$$\mu_3 f_5 = \lambda_3 f_1 \quad (20)$$

$$\mu_4 f_6 = \lambda_4 f_1 \quad (21)$$

$$\mu_5 f_7 = \lambda_5 f_1 \quad (22)$$

$$\mu_1 f_8 = \lambda_1 f_2 \quad (23)$$

$$\mu_2 f_9 = \lambda_2 f_2 \quad (24)$$

$$\mu_3 f_{10} = \lambda_3 f_2 \quad (25)$$

$$\mu_4 f_{11} = \lambda_4 f_2 \quad (26)$$

$$\mu_4 f_{12} = \lambda_5 f_2 \quad (27)$$

$$\mu_4 f_{13} = \lambda_7 f_2 \quad (28)$$

By recursively solving these equations, we obtain

$$f_2 = Gf_1, \text{ where } G=\frac{\lambda_6}{\lambda_7} \quad (29)$$

$$f_3 = \frac{\lambda_1}{\mu_1} f_1 \quad (30)$$

$$f_4 = \frac{\lambda_2}{\mu_2} f_1 \quad (31)$$

$$f_5 = \frac{\lambda_3}{\mu_3} f_1 \quad (32)$$

$$f_6 = \frac{\lambda_4}{\mu_4} f_1 \quad (33)$$

$$f_7 = \frac{\lambda_5}{\mu_5} f_1 \quad (34)$$

$$f_8 = \frac{\lambda_1}{\mu_1} Gf_1 \quad (35)$$

$$f_9 = \frac{\lambda_2}{\mu_2} Gf_1 \quad (36)$$

$$f_{10} = \frac{\lambda_3}{\mu_3} Gf_1 \quad (37)$$

$$f_{11} = \frac{\lambda_4}{\mu_4} Gf_1 \quad (38)$$

$$f_{12} = \frac{\lambda_5}{\mu_5} Gf_1 \quad (39)$$

$$f_{13} = \frac{\lambda_6}{\mu_6} Gf_1 \quad (40)$$

Presently, by use of the standardizing condition

$$f_1+f_2+f_3+f_4+ \ldots + f_{13}+= 1 \quad (41)$$

We get

$$f_1 = [(1+\frac{\lambda_1}{\mu_1} + \frac{\lambda_2}{\mu_2} + \frac{\lambda_3}{\mu_3} + \frac{\lambda_4}{\mu_4} + \frac{\lambda_5}{\mu_5}) (1+G) + \frac{\lambda_6}{\mu_6}] \quad (42)$$

The long run availability of the system A (∞) can now be calculated by formula,

$$A(\infty) = f_1 + f_2$$

$$= (1+G) f1 \quad (43)$$

9. A Study of Behavior

9.1 A State of Transience

The system's dependability, as delineated in equation (15), has been calculated for many combinations of repair and failure rates. It should be noted that these combinations are not exhaustive, as we have only examined the primary subsystems in the numerical analysis. The system's dependability, determined by various combinations of failure and repair rates, is illustrated in Tables 1 through 6. The final row of the data presents the mean time before failure (MTBF) in days corresponding to the respective failure rates. The Mean Time between Failures (MTBF) has been calculated utilizing Simpson's one-third rule.

9.2 Impact of Separator Failure Rate on System Dependability

In terms of mechanics, this substantiates that the cream separator operates as a single-point, high-speed rotational failure: any increase in bearing, seal, or imbalance-related stoppages instantly blocks the flow of cream to every unit downstream. This bowl is used to process all of the product; therefore, even small increases in its failure rate result in a direct reduction in the time the line is available for production. The impact of the sub-system's failure rate on the overall system dependability is evaluated by adjusting its value to $\lambda_1 = 0.006$, 0.007, 0.008, 0.009, and 0.010. The failure and repair rates of further sub-systems are as follows: $\lambda_2 = 0.0005$, $\lambda_3 = 0.00727$, $\mu_1 = 0.41$, $\mu_2 = 0.40$, $\mu_3 = 0.67$, $\mu_4 = 0.33$, $\mu_5 = 0.67$, and $\mu_6 = 6.00$. The system's dependability is determined from these data, yielding a reliability

assessment. The values of α_1 have been examined during the span of days. The system's dependability diminishes by around 0.036% over time. Nonetheless, it decreases by approximately 0.93% when the separator failure rate rises from 0.0006 to 0.010, while MTBF declines by approximately 0.90%.

Table 1: Effect of Failure Rate of Separator on Reliability of the System

$\lambda_1 \rightarrow$ Days ↓	0.006	0.007	0.008	0.009	0.010
30	0.962089	0.959837	0.957596	0.955365	0.953144
60	0.961955	0.959704	0.957464	0.955233	0.953013
90	0.961872	0.959622	0.957381	0.955152	0.952932
120	0.961821	0.959571	0.957331	0.955101	0.952881
150	0.961790	0.959539	0.957299	0.955069	0.952850
180	0.961770	0.959519	0.957279	0.955049	0.952830
210	0.961758	0.959507	0.957267	0.955038	0.952818
240	0.961750	0.959500	0.957260	0.955030	0.952811
270	0.961745	0.959495	0.957255	0.955025	0.952806
300	0.961742	0.959492	0.957252	0.955022	0.952803
330	0.961741	0.959490	0.97250	0.955020	0.952801
360	0.961741	0.959489	0.957249	0.955019	0.952800
MTBF	346.638	345.849	345.066	344.386	343.509

9.3 Impact of the Failure Rate of Condition-Based Maintenance on System Dependability

In terms of mechanics, the CBM functions as a crucial rotating train in the center of the line rather than at its head. As a result, its faults mostly lose capacity after upstream processing has already been completed. As a consequence, increases in the CBM failure rate continue to affect reliability and MTBF negatively, but with a lower impact than the separator. This is because part of the upstream work had already been completed before the halt.

As part of the investigation into the impact of the failure rate of sub-system C on the overall dependability of the system, the values of λ_2 are varied as follows: 0.005, 0.0052, 0.0054, 0.0056, and 0.0058. The calculated failure and repair rates for additional sub-systems are as follows: $\lambda_1 = 0.008$, $\lambda 3 = 0.0027$, $\lambda 4 = 0.0009$, $\lambda 5 = 0.0027$, $\lambda 6 = 0.0055$, and $\lambda 7 = 0.011$. The values of μ_1 is 0.41, μ_2 is 0.4, μ_3 is 0.67, μ_4 is 0.33, μ_5 is 0.67, and μ_6 is 6.00. Table 2 presents the results of the calculation performed with these data to determine the system's level of dependability. This table illustrates how the failure rate of CBM affects the system's dependability for discussion. Taking into account the number of days, the values of λ_2 have been considered. As the time increases from 30 to 360 days, the system's reliability decreases by 0.036%. However, the system's reliability decreases by roughly 0.19% as the CBM failure rate increases from 0.0052 to 0.0058, and the mean time between failures (MTBF) similarly decreases by approximately 0.19%.

Table 2: Impact of CBM Failure Rate on System Reliability

$\lambda_2 \rightarrow$ DAYS↓	0.0050	0.0052	0.0054	0.0056	0.0058
30	0.958743	0.958284	0.957825	0.956366	0.956908
60	0.958610	0.958151	0.957692	0.957234	0.956777
90	0.958528	0.958069	0.957611	0.957152	0.956695
120	0.958477	0.958018	0.957560	0.957102	0.956643
150	0.958446	0.957986	0.957528	0.957070	0.956612
180	0.958426	0.957967	0.957508	0.957050	0.956592
210	0.958414	0.957955	0.957496	0.957038	0.956580
240	0.958406	0.957947	0.957489	0.957031	0.956573
270	0.958401	0.957943	0.957484	0.957026	0.956568
300	0.958399	0.957940	0.957481	0.957023	0.956565
330	0.958397	0.957938	0.957479	0.957021	0.956563
360	0.958396	0.957937	0.957478	0.957020	0.956562
MTBF	345.468	345.306	345.147	344.985	344.826

9.4 Dependability of the System as a Function of Melting Vat Failure Rate

Melting vats are essentially agitated storage with very low-speed drives, thus from a mechanical perspective, their failures often buffer brief disruptions rather than abruptly stopping the whole chain. In contrast to the separator and CBM, the melting vats act more like capacity-smoothing containers than as dominant spinning bottlenecks, as evidenced by the small decline in reliability and MTBF as λ_3 grows.

By changing its values to λ_3 = 0.0022, 0.0024, 0.0026, 0.0028, and 0.0030, the impact of sub-system D's failure rate on the system's dependability is investigated. The following values were used to calculate the failure and repair rates of the remaining subsystems: λ_1 = 0.008, λ_2 = 0.0055, λ_4 = 0.0009, λ_5 = 0.0027, λ_6 = 0.0055, λ_7 = 0.0111, μ_1 = 0.41, μ_2 = 0.40, μ_3 = 0.67, μ_4 = 0.33, μ_5 = 0.67, and μ_6 = 6.00. Table 3 displays the results of the reliability calculation performed on this data. The table below illustrates how the system's dependability is affected by the melting vat failure rate. We have taken the number of days into account while considering the λ_3 values. The table shows that the system's dependability drops by 0.0285% in the first quarter and stays the same in the remaining three months. As the melting vat failure rate increases from 0.0022 to 0.0030, both reliability and MTBF fall by about 0.11%.

Table 3: Impact of Melting Vat Failure Rate on System Reliability

$\lambda_3 \rightarrow$ DAYS ↓	0.0022	0.0024	0.0026	0.0028	0.0030
30	0.958280	0.958006	0.957732	0.957459	0.957185
60	0.958148	0.957874	0.957600	0.957327	0.957053
90	0.958066	0.957792	0.957518	0.957245	0.956971
120	0.958015	0.957741	0.957467	0.957194	0.956920
15	0.957983	0.957707	0.957436	0.957162	0.956889
180	0.957964	0.957690	0.957416	0.957142	0.956869
210	0.957951	0.957678	0.957404	0.957131	0.956857
240	0.957944	0.957670	0.957396	0.957123	0.956850
270	0.957939	0.957665	0.957392	0.957118	0.956845
300	0.957936	0.957663	0.957389	0.957115	0.956842
330	0.957935	0.957661	0.957387	0.957113	0.956840
360	0.957933	0.957660	0.957386	0.957112	0.956839
MTBF	345.306	345.210	345.314	344.018	344.922

9.5 Dependability of the System as a Function of Separator Repair Rate

When it comes to mechanics, quicker separator repair means that bowl, motor, and gearbox interventions can rapidly restore cream flow, thereby reducing the time required for entire line outages. The improvement in reliability and mean time between failures (MTBF) that has been observed as μ_1 grows reflects the significant leverage that design-for-maintainability measures have on this crucial rotating unit, including accessibility, tools, and spare modules.

The impact of the sub-system separator's repair rate on system dependability is examined by varying it to μ_1 = 0.30, 0.35, 0.40, 0.45, and 0.50. The failure and repair rates of the other subsystems are as follows: λ_1 = 0.008, λ_2 = 0.0055, λ_3 = 0.0027, λ_4 = 0.0009, λ_5 = 0.0027, λ_6 = 0.0055, λ_7 = 0.0111, μ_2 = 0.40, μ_3 = 0.67, μ_4 = 0.33, μ_5 = 0.67, and μ_6 = 6.00. The system's dependability is determined using this data, with findings presented in Table 4. The table indicates that the system's dependability improves by 0.36% when the separator's repair rate (μ_1) is elevated from 0.3 to 0.35, with only minimal gains for μ_1 over 0.35. Moreover, dependability decreases by approximately 0.036% as the duration increases from 30 to 360 days. MTBF rises by around 1.0% as the repair rate escalates from 0.30 to 0.50.

Table 4 (a): System Reliability and the Separator Repair Rate

$\mu_1 \rightarrow$ DAYS ↓	0.30	0.35	0.40	0.45	0.50
30	0.951082	0.954538	0.957149	0.959188	0.960827
60	0.950950	0.954407	0.957017	0.959056	0.960694
90	0.950870	0.954326	0.956935	0.958937	0.960611
120	0.950819	0.954275	0.956884	0.958922	0.960560
150	0.950788	0.954244	0.956852	0.958891	0.960528
180	0.950768	0.954224	0.956833	0.958871	0.960509
210	0.950756	0.954212	0.956820	0.958860	0.960496

Table 4 (b): System Reliability and the Separator Repair Rate

$\mu_1 \rightarrow$ DAYS ↓	0.30	0.35	0.40	0.45	0.50
240	0.950748	0.954204	0.956813	0.958852	0.960489
270	0.950744	0.954199	0.956808	0.958847	0.960484
300	0.950741	0.954197	0.956805	0.958844	0.960481
330	0.950739	0.954195	0.956803	0.958842	0.960479
360	0.950738	0.954194	0.956802	0.958841	0.960478
MTBF	342.787	343.997	344.909	345.622	346.220

9.6 A System's Dependability as a Function of the CBM Repair Rate

Enhancing the CBM repair rate reduces downtime for its drive train and augers; however, its location downstream of the separator allows some upstream inventory to mitigate brief interruptions. This elucidates why augmenting μ_2 enhances system reliability, although with a lesser effect than comparable reductions in separator downtime.

By varying its values to $\mu 2 = 0.30, 0.35, 0.40, 0.45$, and 0.50, the study examines the impact of the sub-system CBM repair rate on the system's dependability. The following values have been used for the failure and repair rates of various sub-systems: $\lambda_1 = 0.008$, $\lambda_2 = 0.0055$, $\lambda_3 = 0.0027$, $\lambda_4 = 0.0009$, $\lambda_5 = 0.0027$, $\lambda_6 = 0.0055$, $\lambda_7 = 0.0111$, $\mu_1 = 0.41$, $\mu_3 = 0.67$, $\mu_4 = 0.33$, $\mu_5 = 0.67$, and $\mu_6 = 6.00$. Table 5 displays the results of calculating the system's dependability using this data. The table shows that as the CBM repair rate increases from 0.30 to 0.50, the system's dependability increases by about 0.66 percentage points. Concurrently, there is a 0.036 percentage-point drop in dependability for each day from 30 to 360. From a repair rate of 0.30 to 0.50, MTBF increases by around 0.64%.

Table 5: The Impact of CBM Repair Rate on System Reliability

$\mu_2 \rightarrow$ DAYS ↓	0.30	0.35	0.40	0.45	0.50
30	0.953413	0.955798	0.957596	0.958998	0.959711
60	0.953281	0.955666	0.957464	0.958866	0.959578
90	0.953200	0.95585	0.957382	0.958784	0.959496
120	0.953149	0.955534	0.957331	0.958733	0.959445
150	0.953118	0.955503	0.957299	0.958701	0.959441
180	0.953098	0.955483	0.957279	0.958681	0.959393
210	0.953086	0.955471	0.957267	0.958669	0.959381
240	.953078	0.955463	0.957260	0.958661	0.959374
270	0.953074	0.955458	0.957255	0.958657	0.959369
300	0.953071	0.955456	0.957252	0.958654	0.959366
330	0.953069	0.955454	0.957250	0.958652	0.959364
360	0.953068	0.955453	0.957249	0.958651	0.959363
MTBF	343.603	344.437	345.066	345.556	345.807

9.7 Impact on System Dependability of Melting Vat Repair Rate

Mechanically, extending the repair time of the melting vats primarily influences residence time and flow smoothness, rather than causing an immediate cessation of all rotating machinery. The small variation in reliability with μ_3 suggests that, while these vessels must remain operational, their maintenance strategies are less vital to overall uptime than those of the high-speed separator and CBM.

As part of the investigation into the impact of the repair rate for sub-system melting vats on the system's dependability, the following values of μ_3 are considered: 0.60, 0.65, 0.70, 0.75, and 0.80. It has been determined that the failure and repair rates of additional sub-systems are as follows: $\lambda_1 = 0.008$, $\lambda_2 = 0.0055$, $\lambda_3 = 0.0027$, $\lambda_4 = 0.0009$, $\lambda_5 = 0.0027$, $\lambda_6 = 0.0055$, $\lambda_7 = 0.0111$, $\mu_2 = 0.41$, $\mu_3 = 0.40$, $\mu_4 = 0.33$, $\mu_5 = 0.67$, and $\mu_6 = 6.00$. The results of the calculation that determines the system's dependability are presented in Table 6, which can be used to derive these data. According to the data shown in this table, the reliability and mean time between failures (MTBF) of the system increase by roughly 0.1% when the repair rate of the separator (μ_3) is increased from 0.60 to 0.80. The increase in time from thirty to three hundred and sixty days results in a drop in dependability of around 0.036 percent.

Table 6: Impact of Melting Vat Repair Rate on System Reliability

$\mu_3 \rightarrow$ DAYS ↓	0.60	0.65	0.70	0.75	0.80
30	0.957165	0.957482	0.957554	0.957990	0.958196
60	0.957033	0.957350	0.957622	0.957858	0.958064
90	0.956951	0.957268	0.957540	0.957776	0.957982
120	0.956900	0.957217	0.957489	0.957725	0.957931
150	0.956868	0.957185	0.957457	0.957693	0.957899
180	0.956849	0.957166	0.957438	0.957673	0.957879
210	0.966837	0.957154	0.957426	0.957661	0.957867
240	0.956829	0.957146	0.957418	0.957654	0.957860
270	0.956824	0.957141	0.957413	0.957649	0.957855
300	0.956821	0.957138	0.957410	0.957646	0.957852
330	0.956820	0.957137	0.957408	0.957644	0.957850
360	0.956819	0.957135	0.957407	0.957643	0.957849
MTBF	344.915	345.026	345.114	345.204	345.276

10. Present Status

The effect of change in failure and repair rates of some important sub-systems on the long run availability of the system is studied in this section.

10.1 The Long-Term Availability Impacted by Separator and CBM Failure Rates

The heightened vulnerability of long-term availability to separator failures, in contrast to CBM failures, underscores the separator's position as the primary rotational bottleneck. In mechanical reliability planning, this indicates that decreasing λ_1 via improved balance, lubrication, and bearing management yields a much greater increase in uptime compared to comparable reductions in the CBM failure rate.

In order to investigate the impact of failure rates on the long-term availability of the system, the values of the sub-systems S_1 and S_3 are varied. The values of λ_1 are as follows: 0.006, 0.007, 0.008, 0.009, and 0.010. The values of λ_2 are as follows: 0.0050, 0.0052, 0.0054, 0.0056, and 0.0058. The rates of failure and repair for other subsystems have been determined to be as follows: $\lambda_3 = 0.0027$, $\lambda 4 = 0.0009$, $\lambda_5 = 0.0027$, $\lambda_6 = 0.0055$, $\lambda_7 = 0.0111$, $\mu_1 = 0.41$, $\mu_2 = 0.40$, $\mu_3 = 0.67$, $\mu_4 = 0.33$, $\mu_5 = 0.67$, and $\mu_6 = 6.00$. Utilizing this data, a calculation is performed to determine the system's availability over the long term, and the results are presented in Table 7. The data shown in this table demonstrates that an increase in the failure rate (λ_1) of the separator would have a negative impact of roughly 0.93% on the long-term availability of the system. This is in contrast to the failure rate of the CBM (λ_2), which would only have a negative impact of 0.19% on the availability.

Table 7: The Consequences of the Failure Rates of the Separator and the CBM on the System's Availability Over the Long Run

$\lambda_1 \rightarrow$ $\lambda_2 \downarrow$	0.006	0.007	0.008	0.009	0.010
0.0050	0.962963	0.960675	0.958429	0.956194	0.953969
0.0052	0.962499	0.960189	0.957981	0.955729	0.953514
0.0054	0.962036	0.959268	0.957522	0.955272	0.953060
0.0056	0.961574	0.959268	0.957064	0.954816	0.952606
0.0058	0.961112	0.958808	0.956606	0.954361	0.952153

10.2 Impact of Failure Rates of Separators and Melting Vats on Long-Term Availability

The disparity in availability reduction due to an increase in separator failure rates compared to melting-vat failure rates illustrates their distinct functions in the production line: separator failures promptly incapacitate all downstream units, while melting-vat failures primarily hinder buffering and heating processes. This rating indicates that separator

failure types must be prioritized in root cause investigation and essential spare inventory management.

We have employed fixed failure and repair rates for all sub-systems, except the separator and melting vats, as follows: $\lambda_2 = 0.0055$, $\lambda_4 = 0.0009$, $\lambda_5 = 0.0027$, $\lambda_6 = 0.0055$, $\lambda_7 = 0.0111$, and $\mu_1 = 0.41$, $\mu_2 = 0.4$, $\mu_3 = 0.67$, $\mu_4 = 0.33$, $\mu_5 = 0.67$, and $\mu_6 = 6.00$. The failure rates for the separator and melting vats are as follows: $\lambda_1 = 0.006$, 0.007, 0.008, 0.009, 0.01 and $\lambda_3 = 0.0024$, 0.0026, 0.0028, and 0.0030. The long-term availability of the system is estimated and displayed in Table 8. This table indicates that an increase in the failure rate of separators (λ_1) impacts the long-term availability of the system by roughly 0.93%, while an increase in the failure rate of melting vats (λ_3) affects it by around 0.12%.

Table 8: Impact of Separator and Melting Vat Failure Rates on System Long-Term Availability

$\lambda_1 \rightarrow$ $\lambda_3 \downarrow$	0.006	0.007	0.008	0.009	.010
0.0022	0.962527	0.960216	0.958009	0.955767	0.953542
0.0024	0.962249	0.959940	0.957733	0.955491	0.953269
0.0026	0.961971	0.959633	0.957458	0.955218	0.952996
0.0028	0.961694	0.959387	0.957183	0.954944	0.952724
0.0030	0.961417	0.958111	0.956909	0.954670	0.952452

10.3 Impact of Separator Failure and Repair Rates on Long-Term Availability

The joint sensitivity to λ_1 and μ_1 indicates that the failure rate of the separator and the pace of repair together influence the system's availability. In terms of mechanical dependability, both design strategies that reduce failure rates (enhanced alignment, vibration mitigation, and shaft sealing) and maintenance techniques that expedite repairs (modular assemblies, pre-balanced spare bowls) directly contribute to continuous butter-oil throughput.

We have also computed the system's long-term availability after adjusting for separator failure and repairs. The outcomes of using the following data are displayed in Table 9. The following five levels of separator failure and repair rates have been taken into consideration: $\lambda_1 = 1006$ 0.007, 0.008, 0.009, 0.010 and $\mu_1 = 0.3$, 0.35, 0.40, 0.45, and 0.50. $\lambda_2 = 0.0055$ $\mu_3 = 0.0027$ $\lambda_4 = 0.0009$, $\lambda_5 = 0.0027$ $\lambda_6 = 0.0055$ $\lambda_7 = 0.0111$, and $\mu_2 = 0.4$ $\mu_3 = 0.67$ $\mu_4 = 0.33$ $\mu_5 = 0.67$, $\mu_6 = 6.0$ are the rates for the other sub-systems. Table 9 shows that a higher separator failure rate (λ_1) reduces the system's long-term availability, whereas a higher repair rate enhances it. When the separator's failure rate rises from 0.006 to 0.010, availability falls by 1.2% to 0.7%, and when the separator's repair rate rises from 0.30 to 0.50, availability rises by 0.7% to 1.2%.

Table 9: The Long-Term Availability of the System: The Impact of Separator Failure and Repair Rates

$\lambda_1 \rightarrow$ $\mu_3 \downarrow$	0.006	0.007	0.008	0.009	0.010
30	0.956881	0.953539	0.950816	0.947812	0.944827
35	0.959504	0.956881	0.954272	0.951677	0.949097
40	0.961481	0.959176	0.956881	0.954598	0.952325
45	0.963024	0.960969	0.958920	0.957432	0.954850
50	0.964262	0.962407	0.960558	0.958716	0.956881

10.4 Impact of Melting Vats and CBM Repair Rates on Long-Term Availability

The greater impact of the CBM repair rate relative to the melting-vat repair rate indicates that promptly recovering the continuous butter maker is more crucial for availability than reducing the downtime of the storage vats. This coincides mechanically with the CBM's function as a strongly loaded spinning apparatus facilitating product creation, whereas the vats mainly provide thermal conditioning and retention.

In this area, we have adjusted the CBM and melting vat repair rates as follows: $\mu_2 = 0.3$, 0.35, 0.40, 0.45, 0.50 and $\mu_3 = 0.6$, 0.65, 0.70, 0.75, and 0.80. The following values have been used for the failure and repair rates of the sub-systems: $\lambda_1 = 0.008$, $\lambda_2 = 0.005$, $\lambda_3 = 0.0027$, $\lambda_4 = 0.0009$, $\lambda_5 = 0.0027$, $\lambda_6 = 0.0057$ $\lambda_7 = 0.0111$, $\mu_1 = 0.4$, $\mu_4 = 0.33$, $\mu_5 = 0.67$, and $\mu_6 = 6.00$. Table 10 displays the results of the calculation of the system's long-term availability using these parameters. The long-term system availability is enhanced by both increasing the repair rate of CBM (μ_2) and the repair rate of melting vats, as shown in the table. However, while both rates have an impact on long-term system availability, the former has a greater impact of about 0.7% and the latter of only 0.1%.

Table 10: In the Long Run, the Availability of the System is Affected by the Repair Rates of Both the CBM and the Melting Vats

$\mu_2 \rightarrow$ $\mu_3 \downarrow$	0.30	0.35	0.40	0.45	0.50
0.60	0.952715	0.955081	0.956817	0.958284	0.959387
0.65	0.953032	0.953032	0.957138	0.958605	0.959709
0.70	0.953351	0.955720	0.957458	0.988927	0.960032
0.75	0.953533	0.955902	0.955902	0.959111	0.960216
0.80	0.953714	0.956085	0.956085	0.959295	0.960400

When combined, the sensitivity findings show that the separator and CBM should get the majority of genuine maintenance attention since their reliability and availability are most affected by changes in failure and repair rates. This means that for plant engineers, the melting vats should be treated more like buffer equipment, whose failures are significant but less availability-limiting, and vibration and temperature monitoring, critical spares management, and rapid repair procedures should be given priority for these high-speed rotating units.

11. Conclusion

This research has established a reliability availability framework for a serial butter-oil production line utilizing a Reliability Block Diagram - Continuous Time Markov Chain (RBD CTMC) formulation, wherein the separator (S_1), continuous butter maker (S_2, CBM), and melting vats (S_3) are represented as a repairable mechanical system comprising essential rotating components and auxiliary vessels. By parameterizing the model with subsystem failure and repair rates derived from plant conditions, we have calculated system reliability, mean time between failures (MTBF), and long-term availability, and assessed how variations in the behavior of individual subsystems affect overall line performance. The numerical findings and sensitivity analysis unequivocally indicate that the separator in sub-system S_1 is the principal determinant of system reliability and availability. Within the examined ranges, escalations in separator failure rates result in the most significant declines in reliability, MTBF, and long-term availability, whereas variations in CBM and melting-vat failure rates yield comparatively little impacts. In contrast, enhancing the separator repair rate produces the most significant increases in availability (about 0.7–1.2%) and MTBF (about 1%), while decreases in CBM and melting-vat repair durations lead to relatively modest enhancements. These patterns indicate that maintenance efforts, design-for-service strategies, and spare-parts logistics should be prioritized for the separator train, followed by condition-based monitoring (CBM), while the melting vats should be regarded largely as buffer equipment rather than as availability-limiting spinning gear. The analysis was conducted under the assumptions of exponential time-to-failure and repair, independent component failures, and stationary operating conditions; however, the RBD–CTMC framework can be adapted to accommodate more general lifetime distributions, multistate deterioration, and explicit modeling of maintenance resources, spare parts constraints, and cost–availability trade-offs. The findings offer a quantitative foundation for prioritizing condition monitoring particularly vibration and temperature critical spare parts inventory, and expedited repair protocols for the most significant rotating machinery, thereby directly connecting reliability modeling to daily decisions regarding the design, operation, and maintenance of high-speed mechanical systems in serial food-processing lines.

For mechanical engineering practice, these findings show that plant-wide availability in butter-oil production is primarily determined by the maintainability of the separator train, and that combining targeted design-for-service with SPC-informed mechanical condition monitoring provides a direct, quantitative roadmap for designing, operating, and maintaining high-speed rotating systems in serial food-processing lines.

12. Acknowledgment

we would like to sincerely thank Professor Dr. Sai Kiran Oruganti for his guidance, support, and encouragement throughout this work. His insights and mentorship have been invaluable to our learning and the successful completion of this paper.

References

Baskan, O. (2013). Determining optimal link capacity expansions in road networks using cuckoo search algorithm with lévy flights. *Journal of Applied Mathematics*, *2013*(1), 718015. https://doi.org/10.1155/2013/718015

Buaklee, W., & Hongesombut, K. (2013). Optimal DG Allocation in a Smart Distribution Grid Using Cuckoo Search Algorithm. *ECTI Transactions on Electrical Engineering, Electronics, and Communications*, *11*(2), 16-22. https://doi.org/10.1109/ECTICon.2013.6559624

dos Santos Coelho, L. (2009). An efficient particle swarm approach for mixed-integer programming in reliability–redundancy optimization applications. *Reliability Engineering & System Safety*, *94*(4), 830-837. https://doi.org/10.1016/j.ress.2008.09.001

Eberhart, R., & Kennedy, J. (1995). A new optimizer using particle swarm theory. In *MHS'95. Proceedings of the sixth international symposium on micro machine and human science* (pp. 39-43). Ieee. https://doi.org/10.1109/MHS.1995.494215

Fouad, M. M., Hafez, A. I., Hassanien, A. E., & Snasel, V. (2015). Grey wolves optimizer-based localization approach in WSNs. In *2015 11th International Computer Engineering Conference (ICENCO)* (pp. 256-260). IEEE. https://doi.org/10.1109/ICENCO.2015.7416358

Garg, H., & Sharma, S. (2012). Behavior analysis of synthesis unit in fertilizer plant. *International Journal of Quality & Reliability Management*, *29*(2), 217-232. https://doi.org/10.1108/02656711211199928

Gupta, E., & Saxena, A. (2016). Grey wolf optimizer based regulator design for automatic generation control of interconnected power system. *Cogent Engineering*, *3*(1), 1151612. https://doi.org/10.1080/23311916.2016.1151612

Jayabarathi, T., Raghunathan, T., Adarsh, B., & Suganthan, P. N. (2016). Economic dispatch using hybrid grey wolf optimizer. *Energy*, *111*, 630-641. https://doi.org/10.1016/j.energy.2016.05.105

Kamboj, V. K., Bath, S., & Dhillon, J. (2016). Solution of non-convex economic load dispatch problem using Grey Wolf Optimizer. *Neural computing and Applications*, *27*(5), 1301-1316. https://doi.org/10.1007/s00521-015-1934-8

Kohli, M., & Arora, S. (2018). Chaotic grey wolf optimization algorithm for constrained optimization problems. *Journal of Computational Design and Engineering*, *5*(4), 458-472. https://doi.org/10.1016/j.jcde.2017.02.005

Kumar, A., Sharma, S., & Kumar, D. (2013). Performance analysis of repairable system using GA and fuzzy Lambda-Tau methodology. *International Journal of Quality & Reliability Management*, *30*(9), 1017-1032. https://doi.org/10.1108/IJQRM-06-2013-0104

Li, D., & Haimes, Y. Y. (1992). A decomposition method for optimization of large-system reliability. *IEEE Transactions on Reliability*, *41*(2), 183-188. https://doi.org/10.1109/24.257778

Li, L., Sun, L., Kang, W., Guo, J., Han, C., & Li, S. (2016). Fuzzy Multilevel Image Thresholding Based on Modified Discrete Grey Wolf Optimizer and Local Information Aggregation. *IEEE Access*, *4*, 6438-6450. https://doi.org/10.1109/ACCESS.2016.2613940

Long, W., Wu, T., Cai, S., Liang, X., Jiao, J., & Xu, M. (2019). A Novel Grey Wolf Optimizer Algorithm With Refraction Learning. *IEEE Access*, *7*, 57805-57819. https://doi.org/10.1109/ACCESS.2019.2910813

Manikandan, S., Manimegalai, R., & Hariharan, M. (2016). Gene Selection from microarray data using binary grey wolf algorithm for classifying acute leukemia. *Current Signal Transduction Therapy*, *11*(2), 76-83. https://doi.org/10.2174/1574362411666160607084415

Mirjalili, S., Mirjalili, S. M., & Lewis, A. (2014). Grey wolf optimizer. *Advances in engineering software*, *69*, 46-61. https://doi.org/10.1016/j.advengsoft.2013.12.007

Mirjalili, S., Saremi, S., Mirjalili, S. M., & Coelho, L. d. S. (2016). Multi-objective grey wolf optimizer: A novel algorithm for multi-criterion optimization. *Expert Systems with Applications*, *47*, 106-119. https://doi.org/10.1016/j.eswa.2015.10.039

Mosavi, M. R., Khishe, M., & Ghamgosar, A. (2016). Classification of sonar data set using neural network trained by gray wolf optimization. *Neural Network World*, *26*(4), 393. https://doi.org/10.14311/NNW.2016.26.023

Negi, G., Kumar, A., Pant, S., & Ram, M. (2021). Optimization of complex system reliability using hybrid grey wolf optimizer. *Decision Making: Applications in Management and Engineering*, *4*(2), 241-256. https://doi.org/10.31181/dmame210402241n

Ramírez-Rosado, I. J., & Bernal-Agustín, J. L. (2001). Reliability and costs optimization for distribution networks

expansion using an evolutionary algorithm. *IEEE Transactions on Power Systems*, *16*(1), 111-118. https://doi.org/10.1109/59.910788

Uprety, I. (2012). Stochastic analysis of a reheating-furnace system subject to preventive maintenance and repair. *International Journal of Operational Research*, *13*(3), 256-280. https://doi.org/10.1504/IJOR.2012.045664

Verma, S. M., & Chari, A. (1991). Availability and frequency of failures of a system in the presence of chance common-cause shock failures. *Microelectronics Reliability*, *31*(2-3), 265-269. https://doi.org/10.1016/0026-2714(91)90211-O

Wolpert, D. H., & Macready, W. G. (1997). No Free Lunch Theorems for Optimization. *IEEE TRANSACTIONS ON EVOLUTIONARY COMPUTATION*, *1*(1), 67. https://doi.org/10.1109/4235.585893

Zhang, S., Zhou, Y., Li, Z., & Pan, W. (2016). Grey wolf optimizer for unmanned combat aerial vehicle path planning. *Advances in engineering software*, *99*, 121-136. https://doi.org/10.1016/j.advengsoft.2016.05.015